The (mis)alignment of diffusive fluxes in turbulent combustion: DNS analysis and treatment in the Reaction-Diffusion Manifold (REDIM) model

R. Schießl [*,1], V. Bykov[1], U. Maas[1], A. Abdelsamie[2], D. Thévenin[2]

[1]Institut für Technische Thermodynamik, Karlsruher Institut für Technologie (KIT)
[2]Institut für Strömungstechnik und Thermodynamik (ISUT), Otto-von-Guericke-Universität Magdeburg

Abstract

3D DNS data of decaying turbulent non-premixed flames are analyzed with respect to the mutual alignment of the local scalar's gradients. The gradients of species are not aligned with one single direction, but mostly point in different directions, approximately scattering within a 2D space. The significance of this scatter for the REDIM approach is studied by employing DNS-based gradient estimates as a basis to compute REDIMs. REDIMs obtained with a "conventional" and with a 2D-gradient estimate are compared. The difference is insignificant, indicating that for the current conditions of the DNS (low turbulence with a Taylor Reynolds number $Re_\lambda \leq 30$), the multi-directional nature of dissipative transport is not important.

Introduction

The interaction of diffusive transport processes with chemical reaction is an important phenomenon for combustion. Improved insight into the mutual coupling of reaction and diffusive processes is a key for better understanding of combustion phenomena. The term representing diffusive transport via dissipative fluxes in the detailed scalar transport equations finds its correspondence, in various forms, also in reduced, approximate models for combustion.

Typically, in such models the same local direction for the transport of all scalars is assumed. This might be termed "one-dimensional transport" - the local dissipative fluxes of all scalars are aligned with one spatial direction. This direction is, for instance, given by the gradient of mixture fraction in the classical non-premixed flamelet model [1]. Thus, most studies in this field predominantly base their analysis or description solely on the magnitude of transport processes. The key advantage of this simplification is that diffusive processes can be described by one single parameter [1,2].

However, the diffusive fluxes are vector-valued quantities, and their full description therefore requires specification of both magnitude and direction. The importance of the full description increases with the extent of "non-parallelity" of the local gradients.

In this context, it is interesting to check the parallelity of the diffusive fluxes in a practical combustion scenario. Ideally, experiments in flames could be used for this. However, the analysis would require instantaneous, spatially resolved three-dimensional fields of multiple scalars (ideally, of all species, pressure and temperature) to be measured. This is beyond the currently available capabilities of measurement equipment.

In this work, we consider instead data samples from three-dimensional Direct Numerical Simulations (DNS) of turbulent non-premixed flames. The mutual alignment of diffusion flux vectors of different variables is studied. To this end, a method for gradient analysis, including a quantification of the misalignment of local gradient vectors for different scalars, is introduced and applied to the DNS data set. The extent of the directional scatter of gradients (and therefore, of diffusive fluxes) is found to be considerable. Remarkably, the scatter is not fully random, but approximately restricted to only two spatial dimensions.

This indicates that at least two directions would be needed for a full description of the local diffusive fluxes. Our analysis of DNS data also offers a local hierarchical decomposition of the directions for diffusive transport, based on a singular value decomposition (SVD) of the local gradient vectors. This establishes a hierarchy of the local gradients (and therefore also of the diffusive fluxes) into a principal direction and secondary directions along which diffusive transport proceeds.

These observations have potential significance for simplified computational models, since here mostly only a locally one-dimensional diffusive transport is provided.

In order to assess the significance of the multi-dimensional transport for turbulent combustion regimes, the results of the DNS data analysis are incorporated into the REDIM approach [3] as DNS-based gradient estimates. In the REDIM method, one-, two- and three dimensional gradient estimates can generically be accounted for [3, 4]. REDIMs are then computed for identical boundary conditions, but with the different gradient estimates. Both the observed principal and secondary gradient components from the DNS analysis are used, either separately or in combination. Differences between the two REDIMs are discussed.

Methodology

2.1. DNS data

DNS results were obtained by mean of the highly parallel, three-dimensional in-house DNS code "DINOSOARS". DINOSOARS is a low Mach number

[*] Corresponding author: robert.schiessl@kit.edu

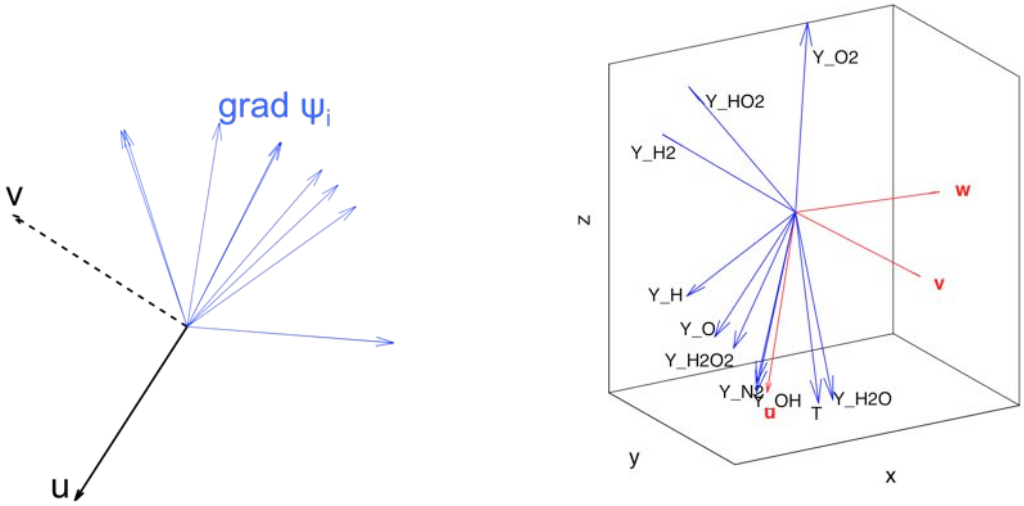

Fig. 1 Left: Some synthetic normalized gradient vectors (simplified example in two dimensions), and the first column u (principal direction) and second column v (secondary direction) of the matrix Y resulting from the hierarchical decomposition via SVD. Right: A three-dimensional example of actual gradients from the DNS data set. Normalized gradient vectors of different species and temperature (as indicated by the labels) are shown along with the three principal direction vectors u, v, w. The gradients are not well-aligned, but scatter approximately within a two-dimensional space.

solver using a 6th order finite difference scheme for spatial derivatives and a 4th order explicit Runge-Kutta scheme for time integration. The chemistry production source term is integrated by the implicit point-wise integrator "RADAU-5" in order to increase the simulation time step. The Poisson equation is solved by an in-house spectral parallel Poisson solver based on the FFTW library, compatible with homogenous and non-homogenous boundary conditions. All kinetic and transport properties in DINOSOARS are handled using Cantera 1.8 and Eglib 3.4. More details concerning the employed DNS method and the governing equations are given in [5].

In the current work, the DNS considers a decaying turbulent non-premixed flame at atmospheric pressure, where diluted N_2/H_2 (75%/25% by mole) counter-flows against an air stream (79%N_2, 21%O_2 by mole), both at 298 K. The detailed chemistry scheme of [6] is used with a simplified Le=1 assumption for molecular transport. This approximation was employed in this first analysis to avoid additional complications associated with effects like differential diffusion.

The computational domain has a size of 3.4 x 10 x 6.8 mm^3, with a spatial resolution of 23, 25 and 25 micrometer, respectively. The time step was fixed at 0.1 µs. The DNS are initialized with species- and temperature profiles from a laminar one-dimensional flame simulation, which are then extended along the 3D geometry. A velocity field corresponding to artificial turbulence, with a Taylor Reynolds number Re_λ=30, large eddy turn-over time τ_Λ=0.32 ms and fluctuation u'=2,1 m/s is then overlaid. The Kolmogorov length and time scales are fully resolved in the DNS simulation. The resulting turbulent flame features local extinction, but is globally burning in a stable manner, as indicated by the temporal evolution of the heat release rate.

2.2. Analysis of gradients

The DNS data set delivers spatio-temporal fields of (among others) the state variables temperature T and n_s species mass fractions Y_i ($i = 1,\ldots,n_s$), comprising a $n_\psi=(n_s+1)$-dimensional state vector $\psi=(T, Y_i)$ at each spatial and temporal point. To analyze the strength and relative orientation of the n_ψ different scalars' gradients, for each time step of the DNS data set, 5000 random points were selected from regions where the heat release rate was at least a specified fraction of the global maximum heat release. Several thresholds were used in different runs of the analysis, ranging from 10^{-6} to 10^{-1}. At each one of these points, the 3D spatial gradients for all scalars were determined. The resulting gradients were arranged into a 3-by-n_ψ gradient array G, in which columns correspond to variables and rows correspond to spatial directions (x, y, z). Normalizing all columns of G to 1 then yields a normalized version G^{norm} of G. We are interested in the mutual (mis-)alignment of the gradient vectors in G or G^{norm}, as opposed to the "overall" direction of the gradients dictated by the local flame orientation. To determine and remove the overall trend, a local coordinate frame that is aligned with the dissipation field is constructed, and the analysis then focuses on the components of the gradients in this aligned frame.

Several methods exist for constructing such a locally aligned coordinate system. For instance, the gradients of selected species or other state variables may be used as a basis for the coordinate system. The classical non-premixed flamelet model [1] employs the gradient of the mixture fraction for this purpose.

In this paper, we take a different approach, searching for the direction that best represents the trend of the different local gradient vectors. For this, the matrix G^{norm} is decomposed according to singular value

decomposition (SVD, [7]) into the matrix product of three matrices A, S and B according to:

$$G^{norm} = A \cdot S \cdot B^{T},$$

where the superscript "T" denotes matrix transposition. The column vectors of the 3x3 matrix A form an orthonormal basis in geometrical space, which is optimally aligned with the directions of the local gradient vectors in G^{norm}. The two-dimensional example in Fig. 1 (left) illustrates this, while the diagram on the right shows a genuine example for the vectors extracted from a point of the DNS. The first column (named u) of A is optimally aligned with the direction of the gradient vectors. The second column (v) in A optimally describes the direction of the gradient vectors after their u-component has been removed, while the third column (w) of A represents the direction that is least represented by the gradient vectors. The column vectors in A = (u v w) therefore constitute a "dissipation-aligned" orthogonal coordinate system, which additionally offers a natural hierarchy of gradient directions.

The matrix S is a diagonal matrix with real positive entries σ_i, (called singular values) which appear sorted (from large to small) along the diagonal (top left to bottom right) of S. The *i*-th singular value represents the importance of the i-th column vector in A for the description of the vectors in G^{norm}. Since $\sigma_1>\sigma_2>\sigma_3$, this reflects the hierarchical ordering of the vectors u,v,w in A. Figure 2 shows, as an exemplary result from the DNS data analysis, the fields of temperature (center) and of the ratio $\sigma_2/(\sigma_1+\sigma_2)$ (right part of the image) in a typical turbulent flame region. Significant regions exist in the flame where the ratio approaches the value 0.5 (the maximum possible value, since $\sigma_2<\sigma_1$), i.e., where the local gradient vectors are close to the maximally possible misalignment.

For our analysis, the Matrix B is of minor interest.

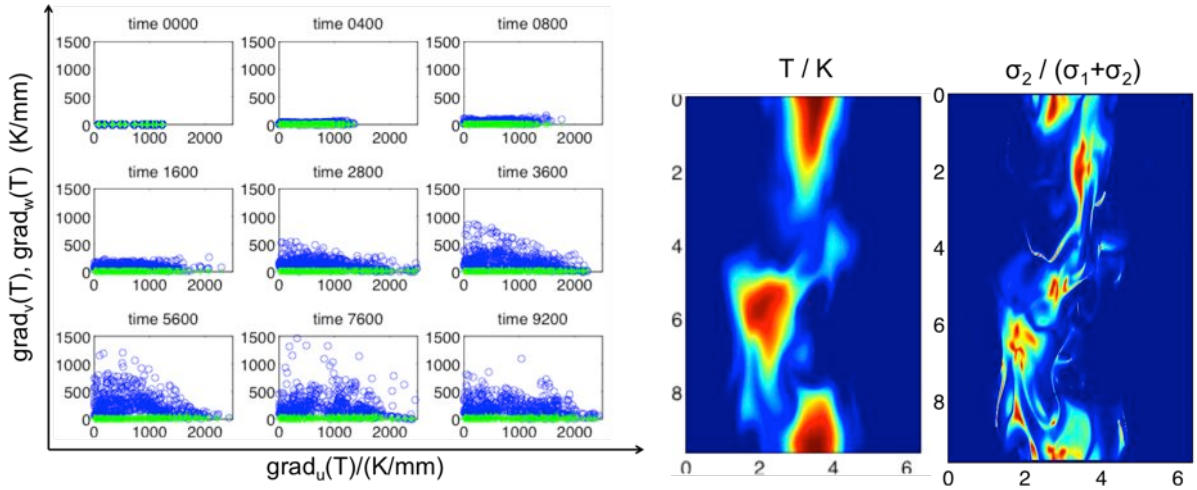

Fig. 2: Left: Temporal development of the u-,v- and w-components of grad(T). Time steps are given in units of 0.1 microseconds. Center: 2D-cut through the temperature field from the DNS sample, showing a turbulent flame (false color scale from 300 K to 1350 K). Right: the ratio $\sigma_1/(\sigma_1+\sigma_2)$ of singular values (false color scale from 0 to 0.5) from the SVD. In some regions within the flame, the ratio is close to the maximum possible value of 0.5, indicating extremely strong local directional scatter of scalar gradients. The x- and y-axes in the central and right diagram are in scales of mm.

By applying the unitary transformation $A^T \cdot G^{norm}$, the coordinates of the variables' gradients in the standard (x,y,z)-coordinate frame are transformed into the coordinates in the dissipation-aligned (u,v,w) coordinate system. These (u,v,w)-based coordinates of gradients will be considered in the sections below.

2.3. Modified REDIM method

In order to illustrate how multi-dimensionality of the system gradients can be accounted for, an overview of the REDIM method will be shortly given in this subsection (see e.g. [3,4] for details). The original system of equations governing the reacting flow can be cast in vector form in coordinate free formulation as the following

$$\frac{\partial \psi}{\partial t} = F(\psi) - \vec{v}\,\mathrm{grad}\,\psi + \frac{1}{\rho}\mathrm{div}\left(D(\psi)\,\mathrm{grad}\,\psi\right) \qquad (1)$$

This system describes the evolution of the thermo-chemical state vector $\psi = (\psi_1,...,\psi_n)$ in time and in physical space, where the ψ_j represent such quantities as the pressure of the mixture p, the enthalpy h and chemical species' specific mole numbers Y_i / M_i, $i = 1,...,n_s$ (mass fractions divided by molar masses). F represents the chemical source term, $\vec{\mathbf{v}}$ is velocity vector, ρ is the density and D is the general diffusion matrix. A reduced model can be created by assuming existence of internal relations (correlations) between the variables of the system (1) such that the detailed system evolves within a low-dimensional surface (manifold) in the state space spanned by the ψ_j. This manifold then can be explicitly defined and described as

$$M = \{\psi = \psi(\theta) : \theta = (\theta_1,...,\theta_m)\},\ m << n\,. \qquad (2)$$

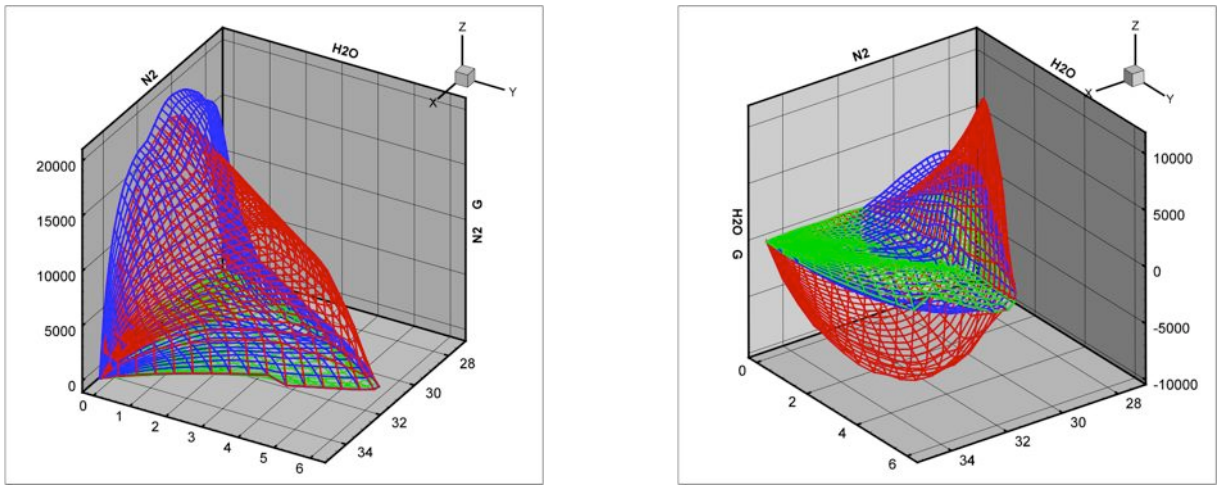

Fig. 3. DNS-based gradient estimates (u- and v-components) on the REDIM manifold as a function of (N_2, H_2O). Blue – grad_U N_2 and H_2O, green – grad_V of N_2 and H_2O, red – gradient estimates taken from linearly extrapolated stationary solutions of the detailed system for different strain rates.

The REDIM equation can be used to find the manifold (surface) resulting from the invariance relations (see e.g. [3,4,8]), by using some initial solution and estimates of the detailed system's gradients as

$$\begin{cases} \dfrac{\partial \psi(\theta,\tau)}{\partial \tau} = \left(I - \psi_\theta \psi_\theta^+\right)\cdot\left[F(\psi(\theta)) + T(\psi(\theta))\right] \\ \psi(\theta,0) = \psi_0(\theta) \end{cases} \qquad (3)$$

$$T(\psi(\theta)) = \frac{1}{\rho}\text{div}\left(D(\psi(\theta))\psi_\theta(\theta)\text{grad}\theta\right)$$

In this approach, the molecular transport term describing the fluxes $\text{div}(D(\psi)\text{grad}\,\psi)$ explicitly depends on the detailed system's gradients calculated on the manifold

$$\text{grad}\,\psi(\theta) = \psi_\theta(\theta)\,\text{grad}\,\theta \qquad (4)$$

Hence, the information on the gradients and their dependence on the reduced variable θ must be specified before the stationary solution of Eq. (3) can be calculated. Note that the reduced system's state space – the manifold in Eq. (2) – is defined by only two processes (reaction and diffusion, see e.g. [3] and Eq. (3)). The gradients in Eq. (4) have to be incorporated consistently with the problem's boundary- and initial conditions. In order to illustrate how the multi-dimensional transport can be accounted for, the transport term is simplified by assuming a constant diagonal diffusion matrix and a Cartesian coordinate system

$$\begin{aligned} &\mathrm{T}(\psi) = \text{div}\left(D(\psi)\,\text{grad}(\psi)\right), \\ &D(\psi) = d\cdot I \Rightarrow \mathrm{T}(\psi) = d\,\text{div}\left(\text{grad}(\psi)\right) \end{aligned} \qquad (5)$$

Thus, the simple Laplacian diffusion term in 3D can be written as:

$$\text{grad}(\psi) = \begin{pmatrix} \text{grad}_x(\psi) & \text{grad}_y(\psi) & \text{grad}_z(\psi) \\ | & | & | \end{pmatrix}$$

$$\Rightarrow \mathrm{T}(\psi) = d\begin{pmatrix} \psi_{1,xx} + \psi_{1,yy} + \psi_{1,zz} \\ \psi_{2,xx} + \psi_{2,yy} + \psi_{2,zz} \\ \dots \\ \psi_{n,xx} + \psi_{n,yy} + \psi_{n,zz} \end{pmatrix}$$

By using the gradient estimate as described in subsection 3.2 below and the definition of the Laplace operator, the transport term (transversal to the tangential space of the manifold), Eq. (5) on the manifold can be further simplified to:

$$\begin{aligned} &\mathrm{T}(\psi(\theta)) = d\,\psi_{\theta\theta}(\theta)\circ\text{grad}(\theta)\circ\text{grad}(\theta) = \cdots \\ &d\,[\text{grad}_x(\theta)^T\cdot\psi_{\theta\theta}(\theta)\cdot\text{grad}_x(\theta) + \cdots \\ &\text{grad}_y(\theta)^T\cdot\psi_{\theta\theta}(\theta)\cdot\text{grad}_y(\theta) + \cdots \\ &\text{grad}_z(\theta)^T\cdot\psi_{\theta\theta}(\theta)\cdot\text{grad}_z(\theta)] \end{aligned} \qquad (6)$$

Hence, the gradients of the parameter on the manifold are only needed to employ the REDIM equation and integrate Eq. (3).

These gradients can be found from the DNS data analysis: In the orthogonal local coordinate system (u, v, w), the gradients $\text{grad}_{(u,v,w)}(\psi)$ are estimated (see Fig. 3), and the information about $\text{grad}_{(u,v,w)}(\theta)$ can be transferred to the local coordinates according to Eq. (4). E.g. for the u-direction, it reads

$$\begin{aligned} &\text{grad}_u(\psi) = \psi_\theta\,\text{grad}_u(\theta) \rightarrow \\ &\text{grad}_u(\theta) = \psi_\theta^+\,\text{grad}_u(\psi(\theta)) \end{aligned} \qquad (7)$$

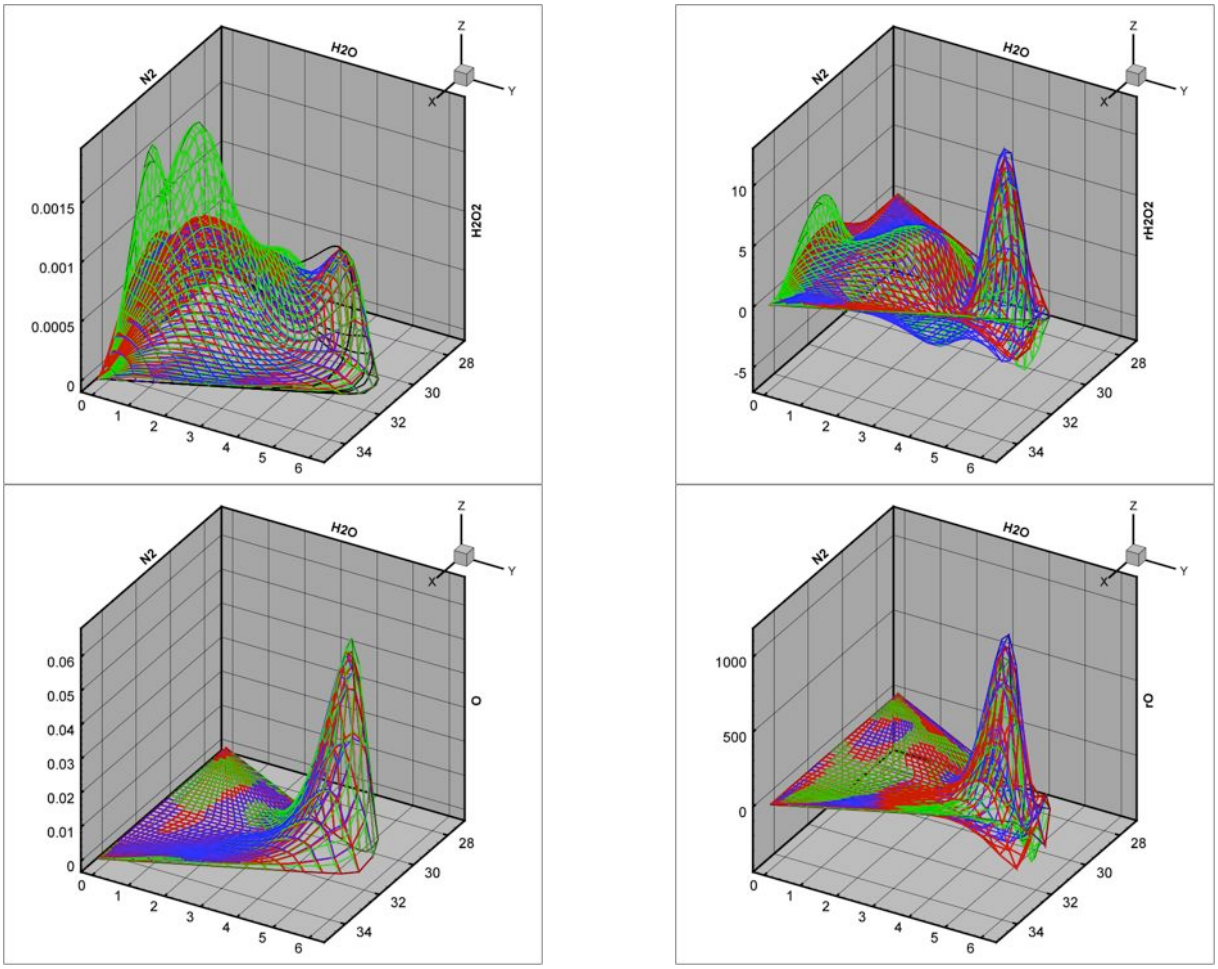

Fig. 4. REDIMs in projection to some species mole numbers. The red mesh shows the REDIM where the transport in both directions u and v was accounted for, blue mesh – only u, green mesh – only v. The black curves are stationary solutions for different scalar dissipation rates.

Results

3.1. Gradient statistics

The directions of gradients corresponding to different variables often scatter strongly (cf. Fig 1). The leftmost diagrams in Fig. 2 show, as a representative data set, the temporal development of the u-, v- and w-components of grad(T) in the flame, as obtained from the DNS data analysis described in section 2.2. The v- and w-components are plotted vs. the u-component. Each of the 9 sub-diagrams refers to one time step of the DNS simulation, as indicated in the labels (times are given in units of 0.1 microseconds). For the initial, laminar flame (time 0), the v- and w- components are zero, reflecting the fact that the gradient of temperature is perfectly aligned with the first principal direction (the u-direction). In fact, for early times, all scalars' gradients are oriented in the same direction, therefore only the u-component is non-zero for all gradients. This corresponds to the case of one-dimensional dissipation, stemming from the one-dimensional flame-based scalar fields used to initialize the DNS. With increasing time, the v-component becomes increasingly important. After 0.36 ms (a time slightly larger than the initial turbulent large eddy turnover time scale, 1.125 τ_Λ) , the magnitudes of u- and v-components become comparable, and two spatial directions now essentially dominate the diffusive transport. Note that the v-component can show the same magnitude as the u-component also for large values of the gradients; the directional scatter is therefore by no means only a spurious phenomenon that occurs only at small, insignificant gradients.

The third (w-) component of the gradient, however, remains small at all timesteps. Although the third dimension (pointing in w-direction) is available in principle, it is practically not represented in the data. Therefore, dissipation here is an essentially two-dimensional phenomenon.

3.2. 1D and 2D gradient estimates

As a result of the SVD-analysis, u, v and w components of gradients are available for 5000 DNS data points, along with the mass fractions of N_2 and H_2O and the corresponding values (θ_1, θ_2). The data points ($\mathrm{grad}_q\psi_k$, q_1, q_2) (q=u, v, k=N_2, H_2O) approximately describe two-dimensional surfaces; numerical

representations of these surfaces were computed on a rectangular grid in the REDIM coordinates (θ_1, θ_2) by taking a distance-weighted average of $\mathrm{grad}_q\psi_k$ at each grid point. Figure 3 shows the resulting surfaces for the u- and v-components of grad N_2 and grad H_2O.

In this way the function of the detailed system solution gradients are estimated and can be incorporated in Eq. (7) e.g. for the first (u-) component:

$$\begin{aligned} \mathrm{grad}_u(\psi) &= f_u(\theta) \rightarrow \\ \mathrm{grad}_u(\theta) &= \psi_\theta^+(\theta) f_u(\theta) \end{aligned} \quad . \tag{8}$$

These estimates can then be used in the integration of the REDIM equation.

3.3. REDIM with 1D and 2D transport

The DNS data analysis provides gradient estimates (see Fig. 3) characterizing the dissipative processes in the considered example as essentially two-dimensional (in the sense of section 3.1). Therefore, the third term in Eq. (6) is negligible, while the second term does have some noticeable contribution (see Fig. 3, compare green and blue meshes). Figure 4 shows the resulting REDIMs for three different cases, together with some stationary detailed solutions of counterflowing flames with different strain rates. For the blue mesh, only 1D dissipation (using grad_u) is accounted for; the green mesh is also for 1D dissipation, but with only grad_v considered in Eq. (7). The red mesh shows the manifold when both grad_u and grad_v are considered in the REDIM evolution equation, Eq. (3). Significant differences are apparent when only the second direction is accounted for (even for main radicals like O or H_2O_2, the maximum concentration is slightly overestimated by the green mesh, see Fig. 4), while the differences between blue and red are moderate. At the same time, Fig. 4 (on the right) shows that the chemical source terms evaluated on the REDIM match much better for both the minor as well as for major species. It additionally gives credits to the 1D model in the example considered here. Namely, it can satisfactorily be described using only one-dimensional dissipation, along the first (u-) direction.

Conclusions

The mutual alignment of the local diffusion fluxes of different state variables (temperature and species) in a non-premixed turbulent combustion scenario has been studied using 3D DNS data. In the considered flame configuration, the local diffusion fluxes of different species display considerable directional scatter, while residing approximately within a two-dimensional subspace of the three-dimensional geometrical space. Such a two-dimensional nature of diffusion fluxes is not accounted for in most simplified combustion models. The significance of the multi-dimensional transport for model reduction was then studied using a REDIM-approach, which naturally allows incorporating these effects. Different REDIMs for identical boundary conditions, but with different dimensionality of the DNS-based gradient estimate were computed and compared. The differences, while noticeable, are quite small.

We conclude that, for the conditions of the DNS considered here (low turbulence level), the two-dimensional dissipative transport is of negligible influence concerning the overall behavior of the reaction-diffusion system. However, for stronger turbulence ($\mathrm{Re}_\lambda \geq 60$, leading to high mixing and dissipation rate) or when more detailed models for molecular transport are used, the multi-dimensional transport might rapidly gain importance as an influencing factor. The methodology developed in this work will be applied to corresponding data with higher turbulence and with more complex diffusion models in the near future.

Acknowledgements

All DNS computations were carried out on the Linux cluster “Karman” at Magdeburg University in the group of Prof. Thévenin. Financial support by the DFG within the German–Israeli Foundation under Grant GIF (No: 1162-148.6/2011) is gratefully acknowledged.

References

[1] N. Peters, Proc. Comb. Inst. 21 (1987) 1231–1250.

[2] J.A. van Oijen, L.P.H de Goey, Combustion Theory and Modelling (CTM) 6 (2002) 463–478.

[3] V. Bykov and U. Maas, Combustion Theory and Modelling (CTM) 11(6) (2007), 839–862.

[4] V. Bykov and U. Maas, Proc. Combust. Inst. 34 (1) (2013) 197–203.

[5] Abdelsamie, A. and Thévenin, D., in Direct and Large-Eddy Simulation IX, (Fröhlich, J., Ed.), Dresden, 62-63 (2013).

[6] Maas, U. and J. Warnatz, Combustion and Flame 74 (1988) 53-69.

[7] G. Golub and C. van Loan 1996. Matrix Computations: Johns Hopkins University Press.

[8] A.N. Gorban, I.V. Karlin and A.Yu. Zinovyev, Physics Reports 396 (4-6) (2004) 197–403.